C. R. Palevol 18 (2019) 236–250

Contents lists available at ScienceDirect

Comptes Rendus Palevol

www.sciencedirect.com

Human Palaeontology and Prehistory (Prehistoric Palaeontology)

A new method of three-dimensional morphometry for analyzing the functional potentialities of bifaces. Contribution to the study of artefacts from AU P3 from the "Caune de l'Arago" (France)

Une nouvelle méthode de morphométrie tridimensionnelle pour analyser les potentialités fonctionnelles des bifaces. Contribution à l'étude des pièces de l'UA P3 de la caune de l'Arago (France)

Cyril Viallet

Université de Perpignan-Via-Domitia/Centre européen de recherche préhistorique, UMR 7194, Histoire naturelle de l'homme préhistorique, 15, rue Victor-Hugo, 66720 Tautavel, France

ARTICLE INFO

Article history:
Received 20 June 2018
Accepted after revision 20 November 2018
Available online 5 February 2019

Handled by Marcel Otte

Keywords:
3D morphometry
Bifaces
Middle Pleistocene
Acheulean

Mots clés :
Morphométrie 3D
Bifaces
Pléistocène moyen
Acheuléen

ABSTRACT

The analysis of the functional potential of bifaces, which are artefacts extending beyond our technical memory, is based on direct (micro-wear) or indirect approaches (experimentation, relationship between form/function, comparative ethnography). Indirect approaches are fundamental when artefacts are not well enough preserved for micro-wear analysis, which is frequent for the middle Pleistocene. This article proposes a new method based on the three-dimensional acquisition of artefact images, enabling us to measure cutting edge angles and depth of cut. This process allows us to distinguish, in particular, between cutting edges created for longitudinal or transverse cutting. The application of this analysis to bifaces from UA P3 of the "Caune de l'Arago" brings to light tools with a high functional potential for longitudinal cutting, some of which were used for incising, others for deep cutting. These results corroborate those obtained by most micro-wear analyses and present new ways of interpreting the functional potential of bifaces.

© 2018 Académie des sciences. Published by Elsevier Masson SAS. This is an open access article under the CC BY-NC-ND license (http://creativecommons.org/licenses/by-nc-nd/4.0/).

RÉSUMÉ

L'analyse du potentiel fonctionnel des bifaces, artefacts hors de notre mémoire technique, résulte d'approches directes (tracéologie) ou indirectes (expérimentation, rapport forme/fonction, comparatisme ethnographique). Les approches indirectes sont fondamentales lorsque la qualité de conservation des artefacts est insuffisante pour développer une analyse tracéologique, un cas de figure fréquent au Pléistocène moyen. Cet article propose une nouvelle méthode basée sur des acquisitions tridimensionnelles des artefacts, permettant de mesurer à la fois les angles de tranchants et les profondeurs de coupe sur lesquels ils

E-mail address: cyviallet@gmail.com

https://doi.org/10.1016/j.crpv.2018.11.001
1631-0683/© 2018 Académie des sciences. Published by Elsevier Masson SAS. This is an open access article under the CC BY-NC-ND license (http://creativecommons.org/licenses/by-nc-nd/4.0/).

s'expriment. Ce procédé permet d'opérer une distinction, notamment, entre des tranchants conformés pour des coupes sortantes ou rentrantes. Appliquée aux bifaces de l'UA P3 de la caune de l'Arago, cette analyse permet de mettre en évidence des outils au fort potentiel fonctionnel de coupe rentrante, certains pour inciser, d'autres pour couper plus profondément. Ces résultats corroborent ceux obtenus en majorité par les analyses tracéologiques et présentent de nouvelles modalités de lecture du potentiel fonctionnel des bifaces.

© 2018 Académie des sciences. Publié par Elsevier Masson SAS. Cet article est publié en Open Access sous licence CC BY-NC-ND (http://creativecommons.org/licenses/by-nc-nd/4.0/).

1. Introduction

Bifaces are well-known artefacts and are frequently used to define the technical and cultural evolution of hominids during the lower and middle Pleistocene, but the functional aspects of these tools are often much less accessible (Boëda, 2013; Ollé et al., 2012).

Microwear analyses focus on the function of lithic artefacts, but they are still rare for middle Pleistocene bifaces, generally due to the preservation status of these artefacts (Beyries, 1993; Marquez et al., 2001). The conclusions of these studies can be summarized as follows:

- the most widely recorded activities are butchery, for cutting actions (García-Medrano et al., 2014; Keeley, 1980; Ollé, 2003), disarticulation (Keeley, 1980) or scraping (Soladenko et al., 2015);
- wood cutting (Binneman and Beaumont, 1992), or wood perforation activities (Keeley, 1980) are also recorded, as well as cutting non-ligneous plant materials (Lhomme et al., 1998);
- the use of bifaces in percussion activities has also been brought to light, instead of hard (Mitchell, 1998; Moncel, 1995; Wenban-Smith and Bridgland, 2001) or medium hard materials (Viallet, 2016a, 2016b), or the ground (Rots and Van Peer, 2006).

However, these analyses concern a limited number of pieces over extremely long time scales and vast areas (the whole Old World during the middle Pleistocene) and therefore it is not yet possible to generalize about the functions of these tools. For this reason, in parallel with micro-wear analyses, it is essential to develop indirect approaches for the study of the functional potential of bifaces.

This type of approach is based on the analysis of the form/function correlation (for a review, see Key and Lycett, 2017b), through experimental studies (Key et al., 2016; Machin et al., 2007) or ethnographic comparativism (Cornford, 1986; Hayden, 2015). In these approaches, forms are generally quantified according to their general and specific dimensions, based on standard classifications (Bordes, 1961; Roe, 1981). The edge angle is a fundamental factor for the functional potentialities of a dihedral section (Lemorini, 1992; Lepot, 1993; Terradillos-Bernal and Rodriguez, 2012); yet it has only rarely been taken into consideration until recently (Key et al., 2016). However, for a given angle, the penetration capacity (in a material) varies according to the depth of cut on which the angle is expressed. In theory, an angle extends over an infinite length. In practice, on a prehistoric or even present-day tool, the edge angle extends until the extremity created by shaping. This length, referred to as depth of cut, has a direct impact on the functional capacities of a cutting edge. These two data — edge angle and depth of cut — constitute the functional potential of a cutting edge and their quantification should thus allow us to compare the functional capacities of different types of biface cutting edges. Ethnographic comparativism and experimental reference collections highlight functioning constants, allowing us to associate functional capacities with movements (Soressi, 2002; Soriano, 2000).

In practice, the measurement of these angles with a goniometer or a calliper is not easy. It is difficult to reproduce the same measurements and the angles of cutting edges cannot be measured with a bi-concave section (Dibble and Bernard, 1980). Recently, several works have used 3D models in lithic studies, with varied aims (*e.g.*, Bretzke and Conard, 2012; Chacon et al., 2016; Clarkson and Hiscock, 2011; Li et al., 2016; Morales et al., 2015). Here, we present the use of three-dimensional biface models to create transversal and longitudinal sections in order to measure edge angles and depth of cut.

Here, this method of functional potential is applied to the bifaces from Archaeostratigraphic Unit (AU) P3 from the "Caune de l'Arago". These bifaces are in a secure stratigraphic context and are associated with abundant lithic and faunal remains. They are among the earliest evidence of bifacial technology in Europe.

2. Materials

The "Caune de l'Arago" (Pyrénées-Orientales, France) is a multi-stratified site in the South of France, comprising several middle Pleistocene lithic complexes (de Lumley, 2015) (Fig. 1A and D). Among these, Unit I, attributed to OIS 14 (Falguères et al., 2015), contains some of the earliest evidence of biface production in Europe, in AU P (Barsky, 2013).

AU P3 is about twenty centimetres deep and was excavated over a surface of less than 80 m^2. It has yielded considerable quantities of archaeological and bone remains, in a good state of preservation (de Lumley, 2015). The lithic assemblage is mainly made in local rocks, associated with artefacts in good-quality flint, chalcedony and jasper materials from further away (> 30 km) (Grégoire, 2000). The debitage is based on (uni- or bifacial) discoid

B

	Lenght (mm)	width (mm)	Thichness (mm)	Proximal part	Distal part	Bilateral balance plan	Bifacial balance plan
F13-1409	63	46	17	Shaped	Raw bevel	No	Yes
G15-8084	86	51	22	Shaped	Tip	Yes	No
E13-2546	80	41	25	Shaped	Retouched bevel	Yes	Yes
F14-3242	74	60	24	Shaped	Retouched bevel	Yes	No
E17-4127	98	57	25	Cortical and shaped	Tip	No	No
E14-2807	69	43	13	Cortical and shaped	Tip	Yes	No
Mean	*78,3*	*49,6*	*21*				
SD	*12,6*	*7,7*	*4,9*				

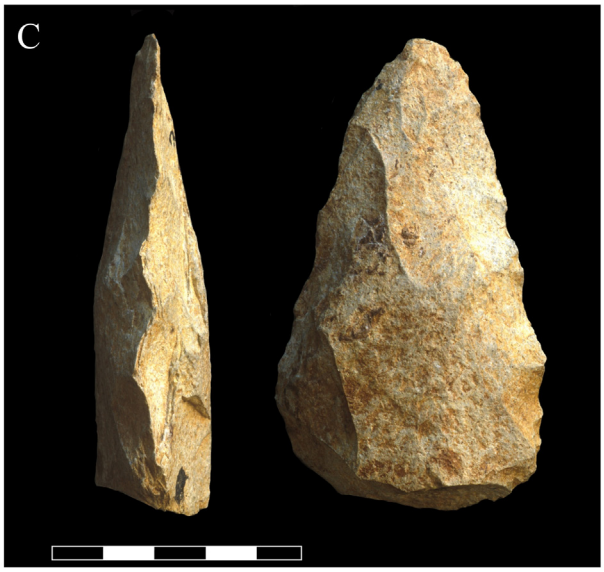

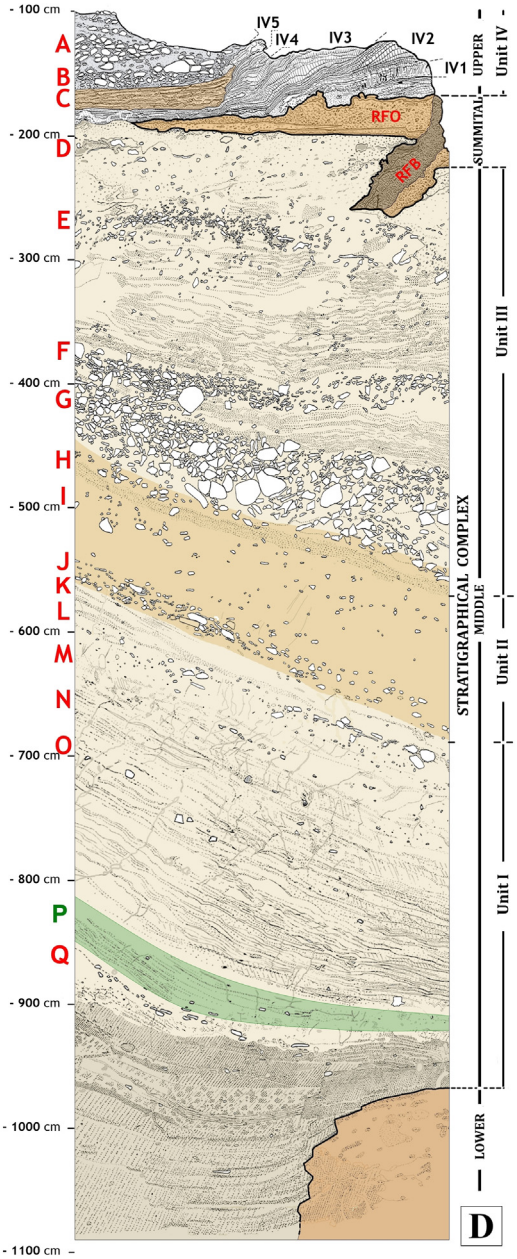

Fig. 1. General presentation of the "Caune de l'Arago". A. Site location, between the Pyrenees Mountains and the Mediterranean Sea. B. Table with the main morphological characteristics of bifaces from AU P3. C. Photograph of one biface from AU P3 (D. Dainat). D. Synthetic stratigraphic column of the "Caune de l'Arago" (C. Perrenoud), with AU P in green.

Fig. 1. Présentation générale de la caune de l'Arago. A. Position du site, à l'interface entre la chaîne Pyrénéenne et la mer Méditerranée. B. Tableau avec les caractéristiques morphologiques principales des bifaces de l'UA P3. C. Photographie d'un biface de l'UA P3 (D. Dainat). D. Log stratigraphique synthétique du remplissage de la caune de l'Arago (C. Perrenoud) avec les UA P en vert.

systems, although more random knapping was also used, producing globular cores. The toolkit consists of points (Tayac, Quinson, Bill Hook) and notches, in addition to pebble tools and bifaces (Fig. 1C) (Barsky, 2013; de Lumley, 2015).

AU P3 contains six bifaces: two in flint and four in sandstone, sandstone-quartzite, quartzite and porphyry (de Lumley, 2015). These artefacts were studied recently as part of a PhD on bifaces in the Southeast of France (Viallet, 2016c). These bifaces are small (*i.e.* less than 10 cm long and 6 cm wide) and were mostly made with a hard hammer stone and in one case with a soft hammer (Fig. 1B). They present deliberate structural imbalances and only one biface shows well-balanced bilateral and bifacial stability *sensu stricto*. Shaping can be facial or lateral and is systematically followed by a finishing phase, which generally

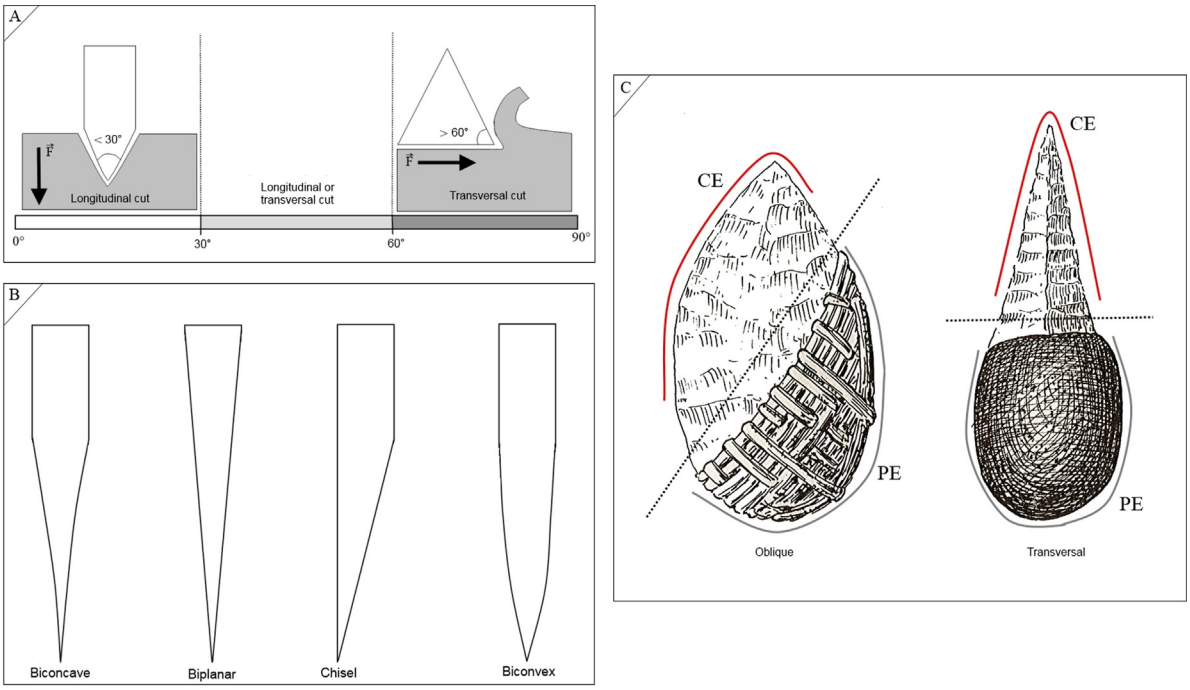

Fig. 2. Functioning constants and operating rationales. A. Sketch showing the link between edge angle and functional potentialities for longitudinal or transversal cutting. B. Sketch of the different morphologies of bevel sections. C. Representation of the two main oppositions between CE and PE.
Fig. 2. Constantes de fonctionnement et logiques opératoires. A. Schéma représentant le lien entre l'angle d'affûtage et le potentiel fonctionnel pour une coupe longitudinale ou transversale. B. Schéma des différentes morphologies de l'émouture. C. Représentation des deux principales oppositions entre unités de contact transformatif et de contact préhensif.

involves sharpening and affects the more convex face. The preservation status of these bifaces is not conducive to the analysis of possible use polish (Raynaud, 2010). There are some scalar chips and rounding, indicating the use of these artefacts in five cases out of six. In one case only, these marks are sufficiently characteristic to suggest the use of the biface for cutting (Viallet, 2016c).

3. Methods

3.1. Theoretical background

The functional hypothesis is based on ethnographic or actualist comparativism, according to the postulate that the universal problems encountered by human populations are equivalent, regardless of the period, and that a similar spectrum of efficient solutions is available (Hayden, 2015). Functional constants and operational rationales are identified based on data from work on the mechanics of cutting movements (Atkins, 2009; Key, 2016; McGorry et al., 2003, 2005; Singh et al., 2016), specific work on the section morphology of (sub-)contemporaneous tools (Boucard, 2005; Cabanié, 1932), experiments on the efficiency of working edges (Key and Lycett, 2015, 2017a) and finally, ethnographic observations generally conducted on Aboriginal hunter-gatherers in Australia (Gould et al., 1971; Hayden, 1977; Schick and Toth, 1993). Two elements are used to propose a functional hypothesis. The first is the type of opposition between the cutting edge and the prehensile edge. The second is the edge morphology in section, referred to in French as the "émouture", or in English as the bevel (Bertrand and Bertrand, 1997; Klaric et al., 2015).

A tool as a system necessarily has an active edge (cutting edge, hereafter CE) and a prehensile zone (prehensile edge, hereafter PE) (Boëda, 2013). These two poles of the tool are opposite each other on the blank, along an axis perpendicular to tool movement (Boucard, 2005; Leroi-Gourhan, 1943). This is illustrated here using the example of Aboriginal bifaces, with known functions (Vayson de Pradennes, 1937) (Fig. 2C). Thus, for longitudinal cutting, the CE/PE pair lies opposite each other along an oblique axis. This is particularly apparent when the cutting edge is associated with a point. In the case of launched percussion and transversal cutting, this opposition is perpendicular (transversally or perpendicularly). However, although this opposition may be transversely or longitudinally perpendicular for transverse cutting, in the case of launched percussion the opposition is usually longitudinal (for elongated and massive tools). Nevertheless, exceptions to those operating rationales do exist (*e.g.*, "couteau à pied", "Ulu"). In addition, several motions can be associated with a single tool (Leroi-Gourhan, 1964; Mansur-Franchomme, 1986). However, the aim here is to highlight recurrent operating rationales, which can then be used to infer hypotheses about the functional structuring of Lower Paleolithic artefacts.

In addition to percussive chopping actions, there are two main types of cutting movements: transverse cutting — to scrape, plane — and longitudinal cutting — to cut, saw or incise. Actualistic sources for transverse cutting show

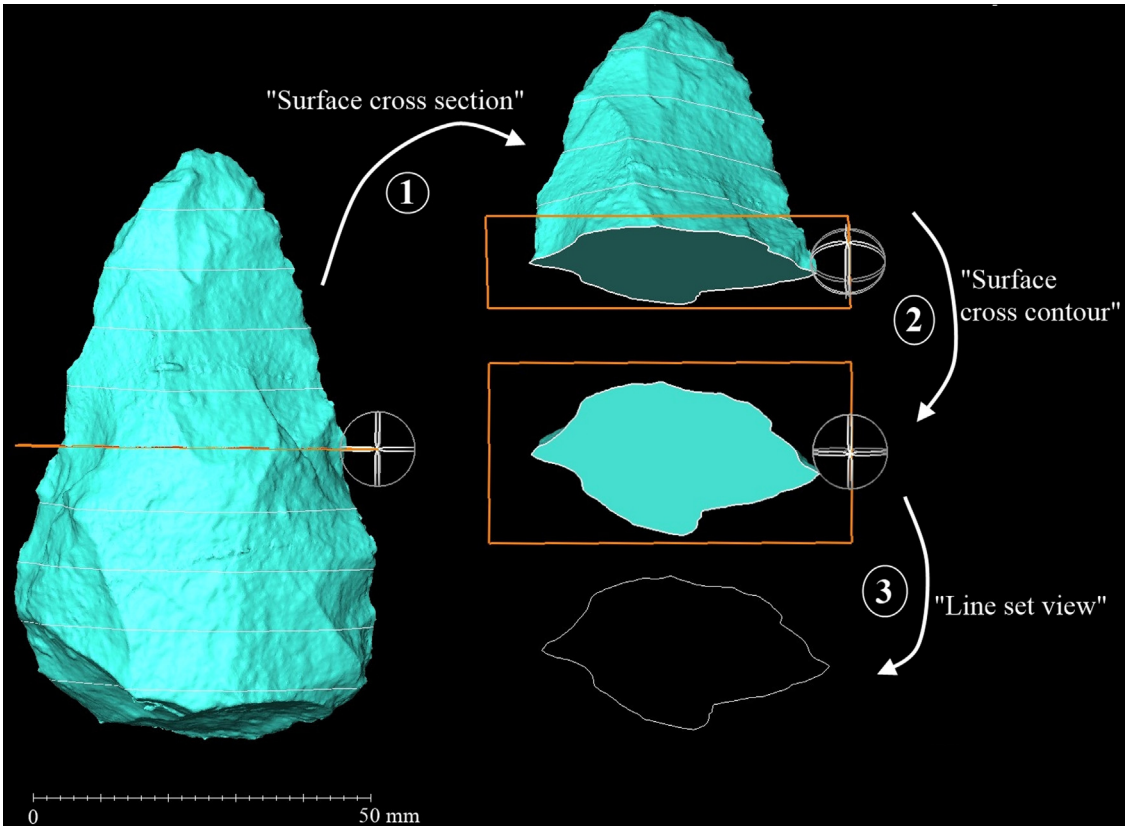

Fig. 3. Representation of the operative chain for the acquisition of the transverse section of a biface with a 3D model.
Fig. 3. Représentation de la chaîne opératoire pour l'acquisition d'une section transversale sur un biface avec un modèle 3D.

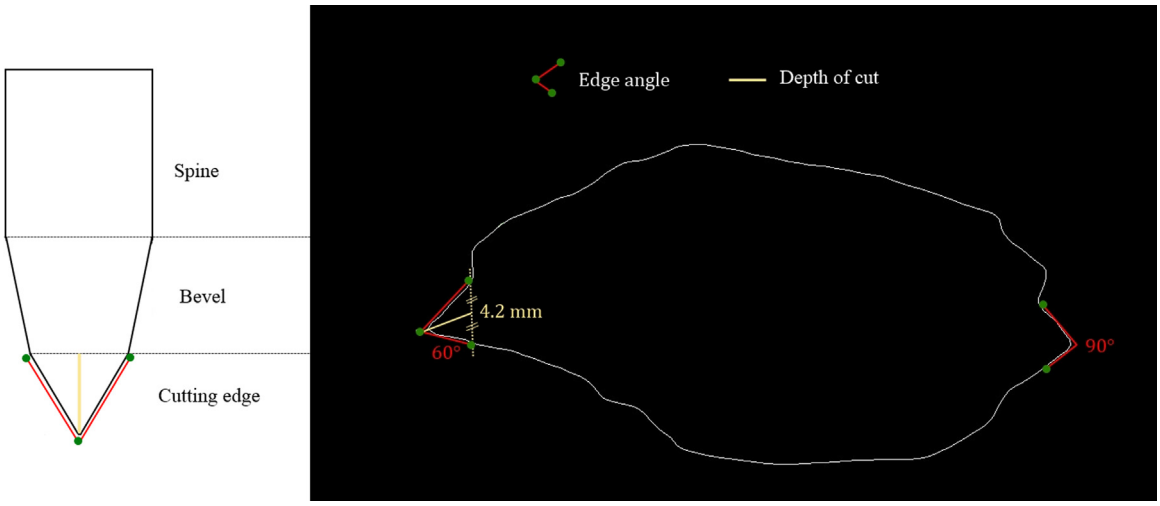

Fig. 4. Terminology used and representation of the edge angle and the depth of cut and their measurement.
Fig. 4. Terminologie utilisée et représentation de l'angle d'aiguisage et de la profondeur de coupe et de leur mesure.

that the angle of the cutting edge can measure up to 60° and its section morphology is asymmetrical (chisel-shaped bevel). Also, the harder the worked material, the higher the angle. In contrast, the cutting edge for longitudinal cutting is less than 60° and is most effective at 30° and the morphology of the section is symmetrical, flat or concave. This latter morphology is the least common, in spite of its efficiency, due to the fragility of the cutting edge. For launched percussion actions, the angle is up to 45° (robustness), and the bevel can be symmetrical (biconvex) or asymmetrical, depending on the associated gesture (Bertrand and Bertrand, 1997; Cabanié, 1932; Geneste and Plisson, 1996;

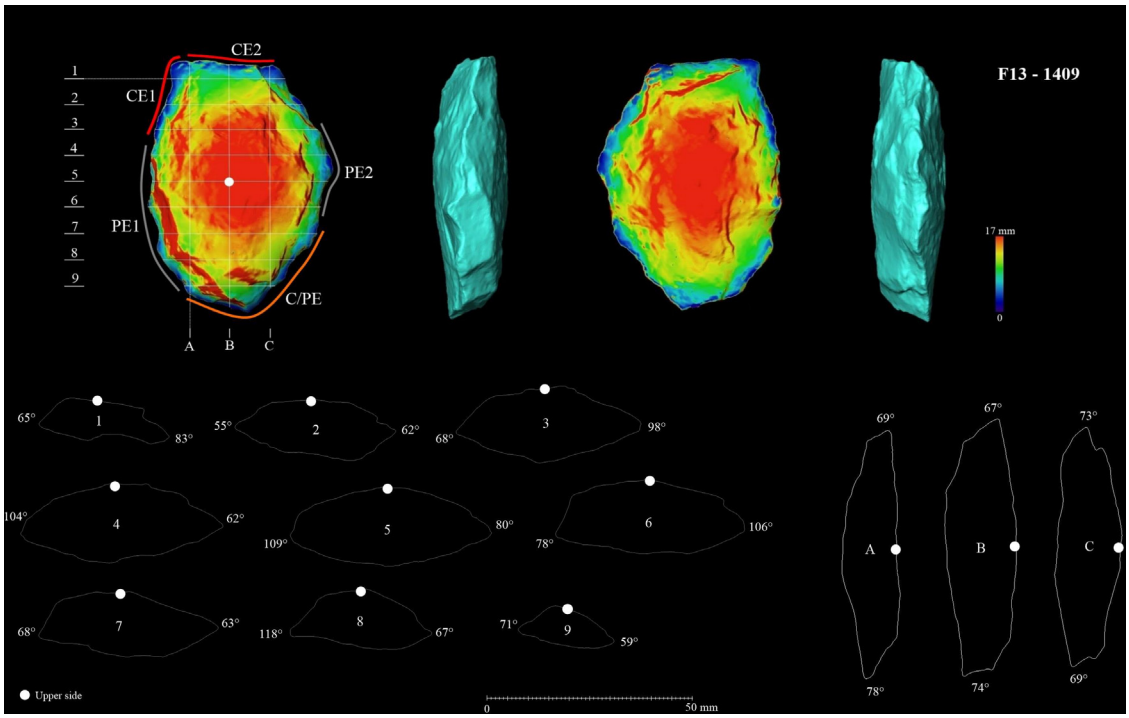

Fig. 5. Biface F13. 1409 – Surface view with colorimetric chart representing variability in tool thickness. Profile view from 3D models. The location of different edge parts is represented by colored lines. Transversal and longitudinal sections and associated edge angle measurements.
Fig. 5. Biface F13. 1409 – La vue des faces avec une carte colorimétrique permet de représenter les différences d'épaisseur de l'outil. Les vues de profil proviennent du modèle 3D. La localisation des différentes parties du bord est représentée par des lignes de couleur. Sections transversales et longitudinales et mesure des angles d'aiguisage.

Gould et al., 1971; Siegel, 1985; Wilmsen, 1968) (Fig. 2A and B). However, these findings are mainly based on metal tools and the angular data of lithic tools are likely to be different. Also, these functional propositions are mere hypotheses. They can only be validated on larger sets of tools.

3.2. Metrical acquisition

A three-dimensional image acquisition program was carried out for the bifaces in order to optimize their conservation (Abel et al., 2011). A portable surface scanner with a maximal precision of 0.1 mm (Créaform Viewscan 3D) was used for digitization. When the 3D model includes small void zones that do not alter our perception of the edges, they are improved with the Géomagic Studio software.

The three-dimensional models are then processed with the Avizo fire 7.1 software. The 3D model is correctly oriented in an orthonormal coordinate system (x, y, and z), so that a virtual section can then be taken along the required axis and direction (Fig. 3). Here, the section is strictly perpendicular to the longitudinal axis in order to obtain a transverse section. This section can then be moved, without varying the longitudinal axis, over the whole length of the biface, in order to observe the evolution of the cutting edges from the base to the point. In the analysis carried out here, transverse cuts were made every centimetre, producing nine cross-sections per biface (because the length of the analysed bifaces was relatively similar — about 10 cm). Three longitudinal cuts were also made to characterize the angles of the proximal and distal parts of the biface.

Edges are described from a qualitative perspective: bevel morphology (simple/double bevel, plane, convex or concave) and cutting edge morphology in profile (straight, scalloped); and quantitative perspective: edge angle and depth of cut. The edge angle (Tringham et al., 1974) is measured between the cutting edge and the first morphological change in the section (which corresponds to the start of the bevel edge). This length corresponds to what we propose to call the depth of cut. This edge angle is associated with the penetration potential, which can be more or less limited, depending on the material. This length is measured in the following way: a straight line is traced from the ruptures in the angles on both surfaces of the edge. The depth of cut corresponds to the distance between the middle of this straight line and the extremity of the edge (Fig. 4).

The depth of cut and the edge angle are measured with Avizo software based on the three-dimensional models. These measurements are then projected onto a bivariate diagram linking the edge angle (on the vertical axis) to the depth of the section (on the horizontal axis). The overall volumetry of the biface is represented by a colorimetric chart, where each colour corresponds to a thickness.

The angle data, the depth of cut and the plan and profile of edge morphology are used to define the edge portions for each biface, which potentially correspond to the CE or PE. These observations then enable us to infer the functional capacities of the edges of the biface.

Table 1
Quantitative and qualitative characteristics of each edge type, for each biface from AU P3.
Tableau 1
Caractéristiques qualitatives et quantitatives de chaque type de bord, pour chaque biface de l'UA P3.

Biface	Types of edges	Edge Angle (°) (min–max)	Depth of cut (mm) (min–max)	Length (mm)	Delineation	Profile	Bevel	Associated prehensile edge	CE/PE opposition	Potential gesture
F13-1409	CE1	55–69	3–4,2	27	Straight/pointed	Scalloped	Biconcave	PE1–PE2	Oblique	Longitudinal cutting
	CE2	67–73	2,9–4,2	31	Straight	Convex	In chisel	PE1–PE2–C/PE	Transverse	Transversal cutting
	C/PE	67–78	0,9–3,7	52	Pointed	Straight	Steep/plane	PE1–PE2	Transverse	Transversal cutting
	PE1	81–111	0,8	46	Convex	Irregular	Steep/plane			
	PE2	90–114	0	33	Irregular	Irregular	Biconvex			
E13-2546	CE1	61–70	2,6–3,4	34	Pointed	Straight	Biplanar	PE1	Oblique	Longitudinal cutting
	CE2	67–70	2,6–3	27	Straight	Straight	Biplanar	PE1	Oblique	Longitudinal cutting
	CE3	52–71	2,3–6,1	48	Convex/pointed	Scalloped	Biconcave	PE2	Oblique	Longitudinal cutting
	PE1	70–103	0–2,3	43	Straight	Irregular	Steep			
	PE2	72–99	0–1,8	42	Convex	Straight	Steep			
E14-2807	CE	37–62	1,3–5,1	84	Convex/pointed	Straight	Convex/plane	PE	Oblique	Longitudinal cutting
	PE	65–101	0–2,4	74	Convex	Irregular	Steep			
E17-4127	CE	35–82	1,3–6,6	118	Straight/pointed	Convex	In chisel	PE1–PE2–C/P1	Oblique	Longitudinal cutting
	PE+	81–84	2,5–3,5	24	Irregular	Scalloped	Biplanar	No specific conformation	Ind.	
	PE1	103–118	0	33	Convex	Ind.	Steep			
	PE2	91–103	0	34	Straight	Ind.	Steep			
F14-3242	CE	54–80	1,4–1,9	32	Pointed	Irregular	Irregular	PE–C/PE1–C/PE2	Tranverse	Transversal cutting
	C/PE1	86–112	0–0,9	43	Notch	Straight	Steep/Plane	C/PE2	Longitudinal	Tranversal cutting
	C/PE2	73–87	0,6–1,5	46	Straight	Straight	Plane/steep	C/PE1	Longitudinal	Transversal cutting
	PE	54–108	0–2,4	90	Convex	Irregular	Irregular			
G15-8084	CE	38–68	2–13,5	84	Straight/convex	Straight	Biplanar	PE1–PE2–C/PE	Oblique	Longitudinal cutting
	PE+	65–75	0,8–4	48	Irregular	Irregular	In chisel	No specific conformation	Ind.	
	PE1	72–106	0–1,3	12	Straight	Irregular	Steep			
	PE2	75–98	0–2,3	74	Convex	Straight	Steep			

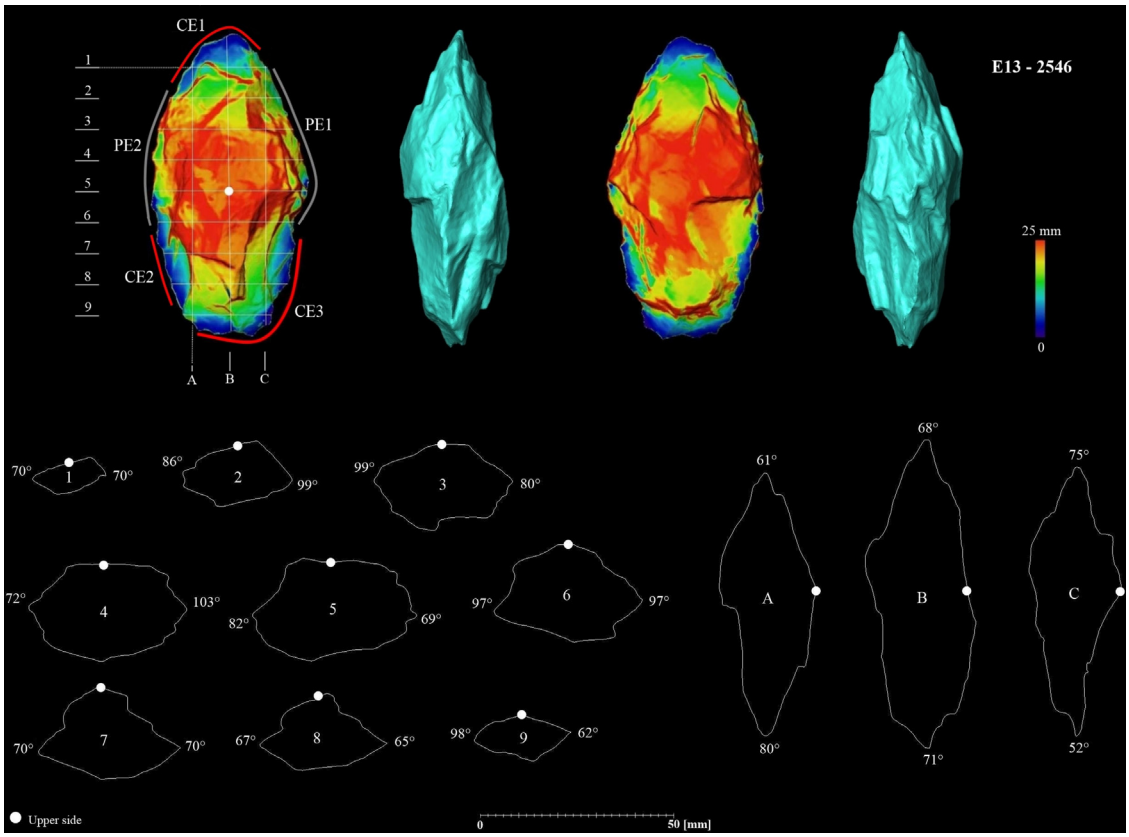

Fig. 6. Biface E13. 2546 – Surface view with colorimetric chart representing variability in tool thickness. Profile view from 3D models. The location of different edge parts is represented by colored lines. Transversal and longitudinal sections and associated edge angle measurements.
Fig. 6. Biface E13. 2546 – La vue des faces avec une carte colorimétrique permet de représenter les différences d'épaisseur de l'outil. Les vues de profil proviennent du modèle 3D. La localisation des différentes parties du bord est représentée par des lignes de couleur. Sections transversales et longitudinales et mesure des angles d'aiguisage.

4. Results

Four edge types were defined for the bifaces from level P3 of the "Caune de l'Arago" based on these qualitative (plan, profile and section morphology) and quantitative (edge angle and depth of cut) criteria. These are PE in nine cases and CE in nine cases. In five cases, these edges are associated with the activation of a CE, and are therefore linked to a prehensile function, but they also present morphological characteristics adapted to use for transverse cutting and remarkable technical intentionality (marked by a retouch phase). They could thus have two functions (*i.e.* CE/PE). When these edges are associated with a specific prehensile zone, this shows their double functional status (F13. 1409; F14. 3242). They are then referred to as bivalent edges and coded C/PE. On the other hand, when there is no associated PE, the polyfunctional status of the edge could correspond either to an archaeological reality or a methodological impasse. Thus, by way of precaution, these zones are only considered prehensile zones for the rest of this analysis. This case occurs twice (E17. 4127; E14. 2807) and coded "PE+".

4.1. Description of the bifaces

F13. 1409 (Fig. 5 and Table 1). On the basis of the measured edge angle and depth of cut, the distal part (between sections A–C) and the left edge (between sections 1–3) can be considered CEs. They correspond to two CEs. CE1 has a scalloped morphology in profile and a biconcave morphology in section, whereas CE2 has a chisel-shaped section and a convex profile. High angles, associated with reduced depth of cut, define two PEs. The first is located between sections 4–9 on the left edge (PE1) and the second between sections 3–6 on the right edge (PE2). Finally, an edge with bivalent functional potentialities (C/PE) is located on the proximal part of the biface (sections A–C and 7–9 of the right edge).

E13. 2546 (Fig. 6 and Table 1). This biface presents 3 CEs and 2 PEs. CE1 is located on the distal part, comprising sections 1 of the left edge and sections A and B. CE2 is on the left edge between sections 7 and 8. It is separated from CE3 on account of the high angle of section 9 on the left edge (and section A on the proximal part). CE3 is on the right edge and the proximal part of the biface, comprising sections B–C

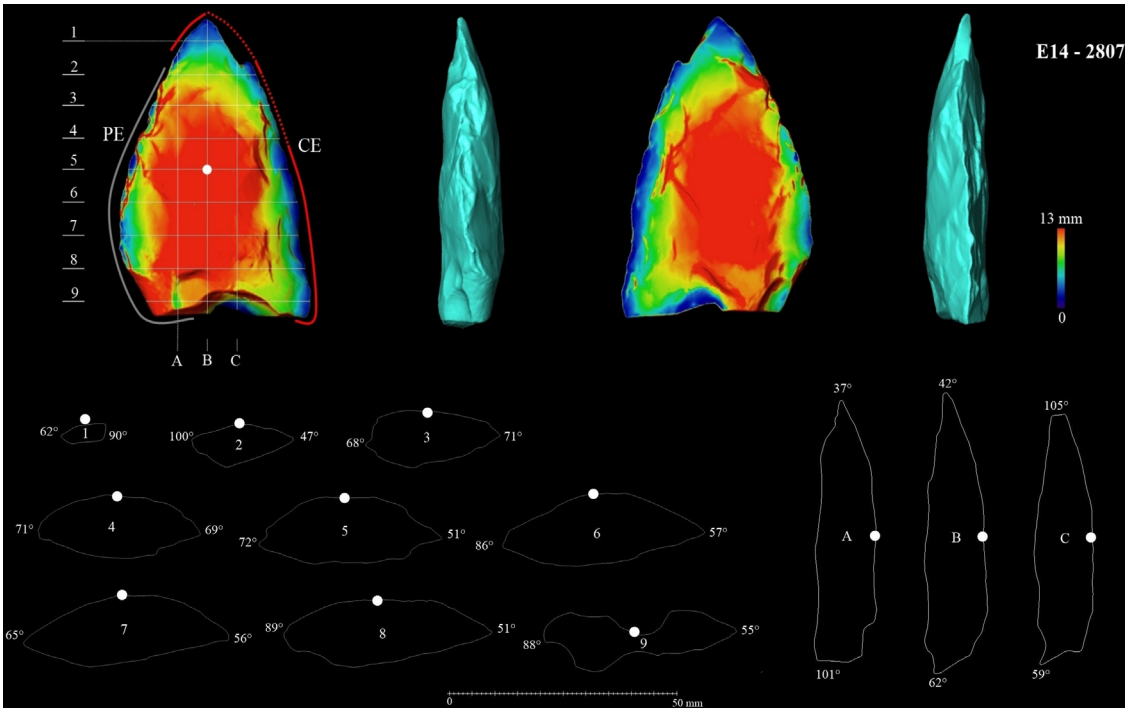

Fig. 7. Biface E14. 2807 – Surface view with colorimetric chart representing variability in tool thickness. Profile view from 3D models. The location of different edge parts is represented by colored lines. Transversal and longitudinal sections and associated edge angle measurements.
Fig. 7. Biface E14. 2807 – La vue des faces avec une carte colorimétrique permet de représenter les différences d'épaisseur de l'outil. Les vues de profil proviennent du modèle 3D. La localisation des différentes parties du bord est représentée par des lignes de couleur. Sections transversales et longitudinales et mesure des angles d'aiguisage.

and 7–9. We identified two areas with very open angles and practically no depth of cut (inexistent or limited), corresponding to PE. PE1 is on the right edge between sections 1–6 and PE2 is on the left edge, between sections 2–6.

E14. 2807 (Fig. 7 and Table 1). A CE and a PE are identified on this biface. The CE corresponds to the right edge, comprising the distal extremity and a small part of the proximal zone (sections 1–9 of the right edge and B–C of the distal part and left edge). The present state of this CE is not homogeneous. Indeed, the distal extremity presents a burin-type fracture with no counter-bulb, indicating that it is not due to a technological action (not intentional). Consequently, this portion of the CE between sections 3–4 on the right edge presents a higher angle than the other parts of the edge, due to a resharpening retouch sequence after the fracture. On the opposite edge and the proximal part, a cortical zone (sections 8–9 of the left edge and A–B of the proximal part) and an abrupt zone constitute a PE.

E17. 4127 (Fig. 8 and Table 1). This biface has an extended CE (118 mm) on the left edge (sections 1-8), the distal extremity (sections A–C) and a small part of the right edge (sections 1–2). This CE is opposed to 2 PE. PE1 corresponds to the right edge, between sections 4–6 and PE2 corresponds to the cortical base, between sections B–C and 9 on the right edge. On the right edge, sections 7 and 8 can be considered as a PE. However, the hypothesis of a CE cannot be totally excluded even if there is no associated prehensile area. Thus, this part of the edge is named PE+.

F14. 3242 (Fig. 9 and Table 1). The distal part of this biface may be a CE. It is technologically shaped by two notches, delimiting a small point. Opposite the point, sections 7–9 of the left edge, 8–9 of the right edge and A–C of the base may correspond to a PE. For the lateral edges, it is not possible to make the distinction between CE and PE on the basis of the measurement of the edge angle and depth of cut. If the right edge is a CE, the left edge could be a PE and vice versa. They are thus bivalent, and are named C/PE1 or 2.

G15. 8084 (Fig. 10 and Table 1). This biface presents a CE on the right edge between sections 1–8, which extends to the distal extremity (sections B and C). On the left distal extremity (sections 1 and A), a small area may be a PE. The principal PE is located on the proximal part, between section 9 of the right edge and section 8 of the left edge. Lastly, the characteristics (angle and depth of cut) of the mesial part of the left edge are bivalent, but it is not associated with a PE, and is thus named PE+.

Linking the edge angles of the CE and the depth of the section on the bivariate diagram highlights the differences in the functional potential of each biface (Fig. 11). A line is plotted at 60° to make a first distinction between longitudinal and transverse sections. We chose to place the limit for the depth of section at 4 mm. For this analysis, this datum appears to distinguish between a shallow (< 4 mm) or deep (> 4 mm) cutting potential. However, it must be applied to a larger quantity of artefacts to grasp the pertinence of this measurement for other analyses.

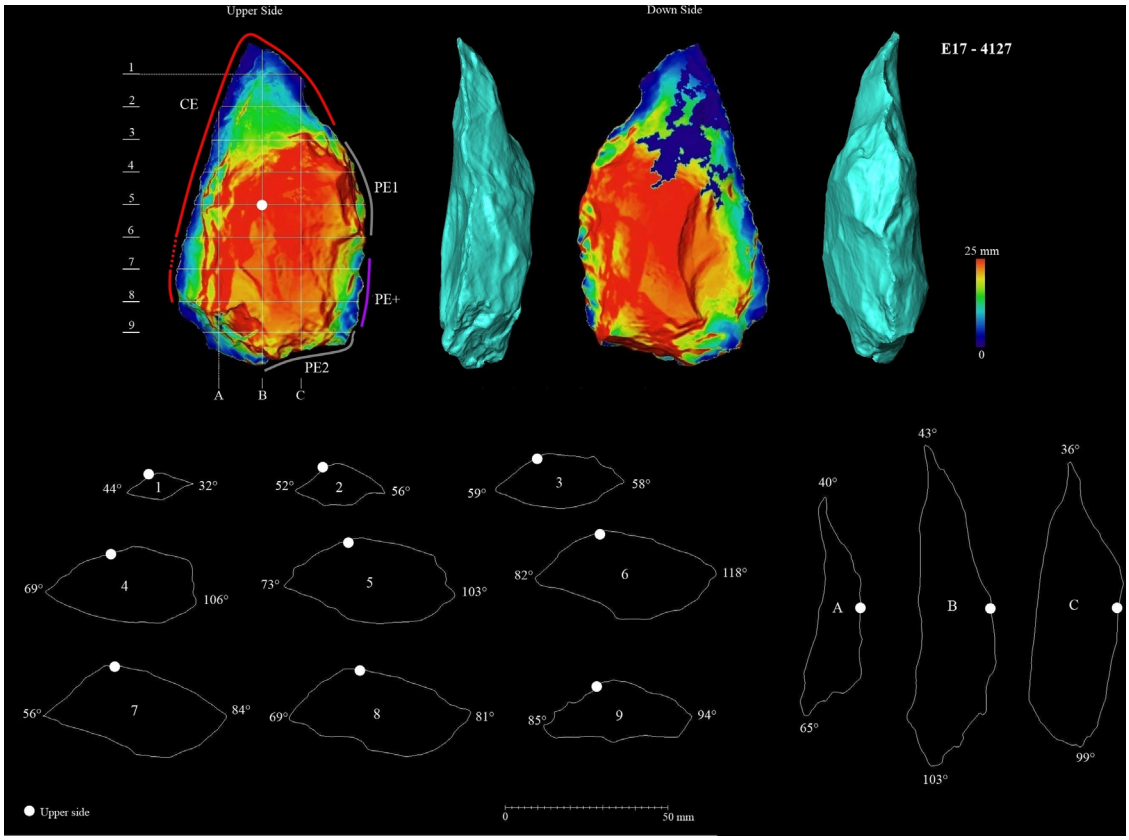

Fig. 8. Biface E17. 4127 – Surface view with colorimetric chart representing variability in tool thickness. Profile view from 3D models. The location of different edge parts is represented by colored lines. Transversal and longitudinal sections and associated edge angle measurements.
Fig. 8. Biface E17. 4127 – La vue des faces avec une carte colorimétrique permet de représenter les différences d'épaisseur de l'outil. Les vues de profil proviennent du modèle 3D. La localisation des différentes parties du bord est représentée par des lignes de couleur. Sections transversales et longitudinales et mesure des angles d'aiguisage.

The five "edge-point"-type CE are divided into three functional groups.

In one case — G15. 8084 — the CE mostly presents angles of less than 60° with a depth of cut of more than 4 mm and a maximum depth of 13.5 mm. The rectilinear morphology of the CE in profile, its symmetrical section, its long length and its oblique association with the PE, characterize a tool with a potential for deep longitudinal cutting.

In two cases — E17. 4127 and E14. 2807 — the CE mostly presents angles of less than 60° and a depth of cut between 1.3 and 6.6 mm. The CEs are regular, rectilinear or slightly convex in profile, with a long section and oblique opposition with the PE. Therefore, these tools were designed for longitudinal cutting. The fact that the depth of cut is often less than 4 mm and the CE section is asymmetric suggest that the edge was intended for a tangential longitudinal cutting motion.

In two cases — E13. 2546/CE3 and F13. 1409/CE1 — the CE present angles of more than 60° and a depth of cut of more than 4 mm. The two CEs present a sharpening retouch phase, creating a scalloped edge morphology in profile and a biconcave morphology in cross-section. The extension of the cutting edge is rather limited. The axis formed with the PE is oblique. Although the angle is more than 60°, the scalloped edge (in profile view), the cross-sectional symmetry and the oblique CE/PE axis are linked to longitudinal cutting motions. The cutting angle of more than 60° of these tools can be explained by the fact that they seem to result from considerable resharpening.

For three bifaces, the angles of certain CEs are more than 60° and the depth of the section ranges between 2 and 4 mm.

In the case of F13. 1409/CE2, the CE is rectilinear in top view and presents an asymmetrical chisel-shaped section. The CE/PE axis is transverse, which corresponds to the configuration of tools used for percussion. However, for this biface, on account of the small dimensions (63 × 46 × 17 mm) and light weight (63 g), we consider that it may have been used for transversal cutting. This is also in agreement with the morphological characteristics of the CE.

The CE1 and CE2 of E13. 2546 are linear or pointed in top view and present a rectilinear profile and a symmetric biplane section, on a relatively short segment of the cutting

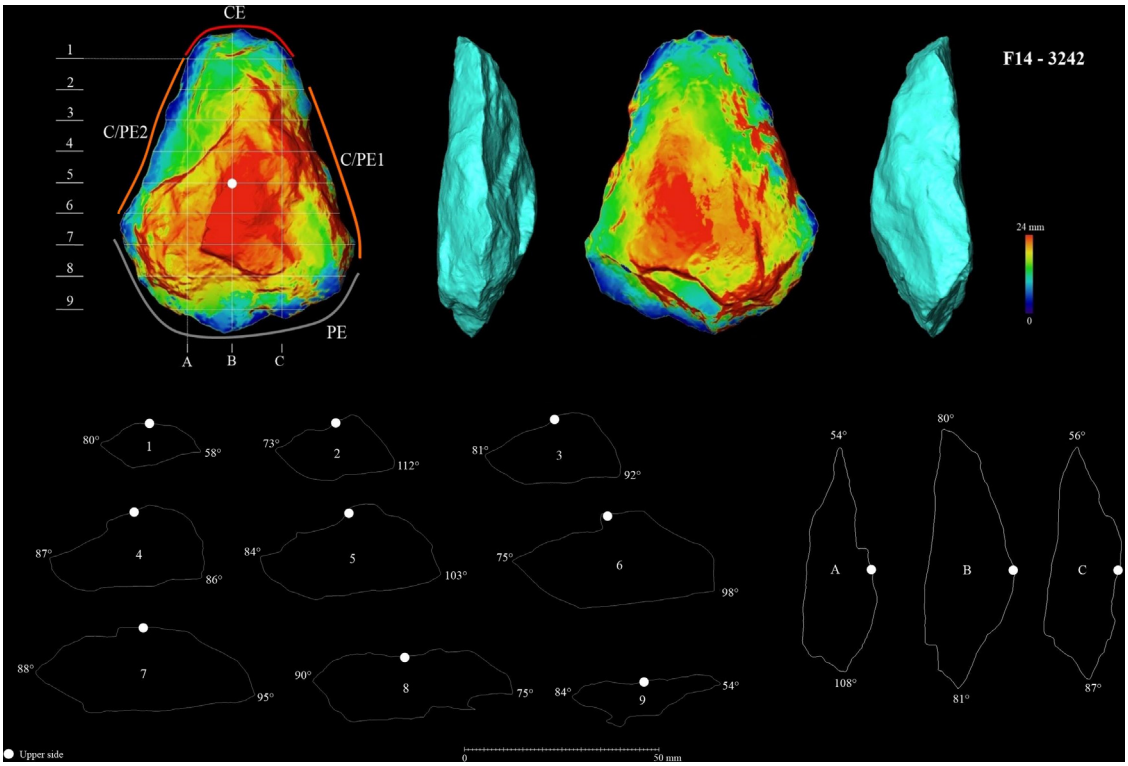

Fig. 9. Biface F14. 3242 – Surface view with colorimetric chart representing variability in tool thickness. Profile view from 3D models. The location of different edge parts is represented by colored lines. Transversal and longitudinal sections and associated edge angle measurements.

Fig. 9. Biface F14. 3242 – La vue des faces avec une carte colorimétrique permet de représenter les différences d'épaisseur de l'outil. Les vues de profil proviennent du modèle 3D. La localisation des différentes parties du bord est représentée par des lignes de couleur. Sections transversales et longitudinales et mesure des angles d'aiguisage.

edge (respectively 34 and 27 mm). The axis with the PE is oblique in both cases. On account of the symmetry and the straightness of the cutting edge and the oblique opposite position of the CE/PE pair, we propose a longitudinal cutting potential, in spite of the high angle (however, the latter is no higher than 70°).

The CE of biface F14. 3242 mostly presents angles of less than 60° and a depth of cut of less than 2 mm. It shows a slightly pointed, short bill-hook morphology, defined by two inverse notches. The axis formed with the PE is transverse. In the same way as for the CE2 of biface F13. 1409, the small dimensions (74 × 60 × 24 mm) and weight of the artefact (112 g) do not suggest use for percussion. This CE/PE pair thus seems to have been used for transversal cutting. This biface also has two edges with bivalent status. These two edges are complementary: when one is a CE, the other is a PE and vice versa; when one is plano-convex in profile, the other is convex-plane.

5. Discussion

The methodology adopted here allowed us to identify nine CEs and three CEs/PEs. Among these, seven display a functional configuration adapted to use for longitudinal cutting. In four cases, the edge angle of these tools is greater than 60°, which is counter to the functioning constants presented earlier (*cf. Methodology*). This allows us to suggest that a longitudinal cutting action is linked to the morphology of the CE, in particular the symmetry in profile of the dihedral section and the oblique axis formed by the CE/PE pair. Consequently, the morphological quantification of bifaces based on the measurement of the angle and the depth of section cannot be considered as an independent method. The acquisition of qualitative data (bevel morphologies in plan or profile; the type of opposition between the CE and PE) are also important for theorizing tool function. Detailed technological analysis is also fundamental: as edge angle progressively increases with resharpening, without necessarily entailing a change in the structure of the tool (straight cutting edge in section and pointed in plan, oblique opposition between the CE and the PE, etc.). The following example illustrates the necessity for combined analysis: among these four longitudinal cutting tools with an angle of more than 60°, three CEs are present on the same biface: E13. 2546. The technological analysis shows that this biface underwent several sharpening sequences and is thus significantly reduced in size. As a result, the high angles of the different CEs can be explained by the intention

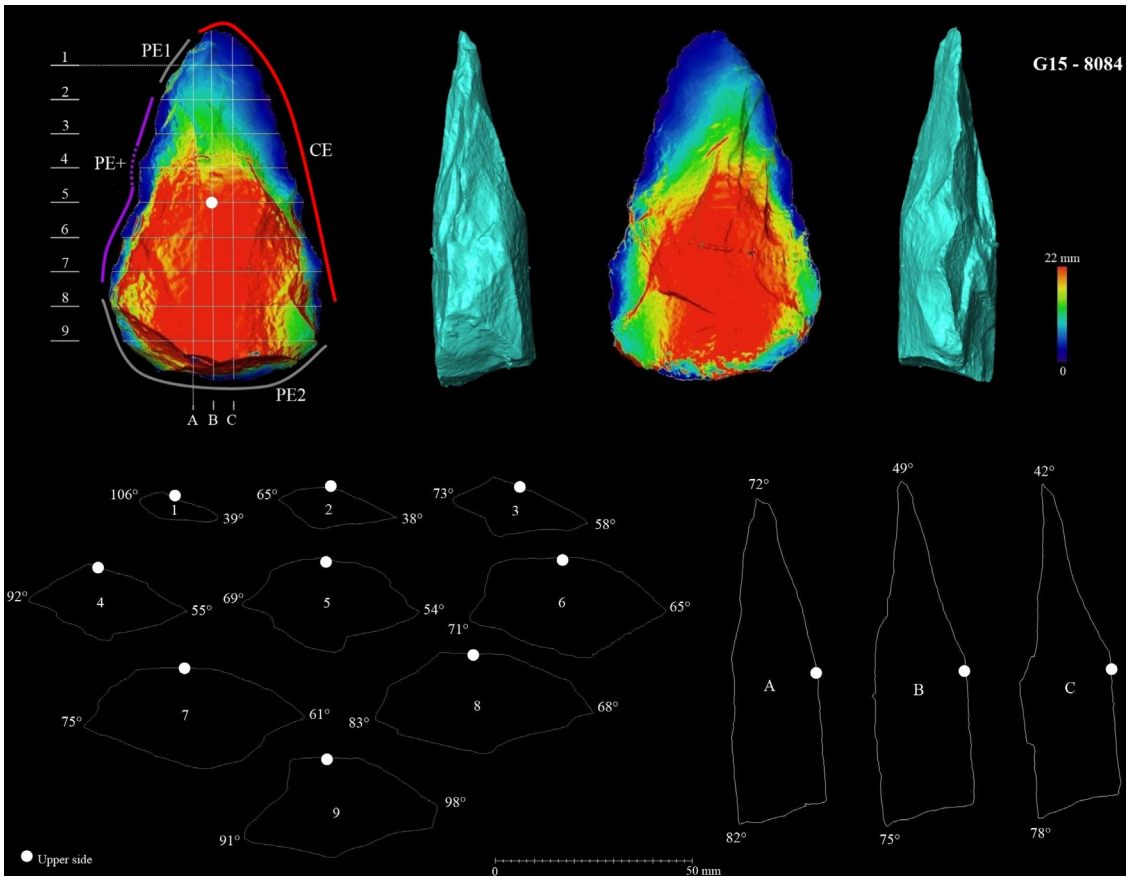

Fig. 10. Biface G15. 8084 – Surface view with colorimetric chart representing variability in tool thickness. Profile view from 3D models. The location of different edge parts is represented by colored lines. Transversal and longitudinal sections and associated edge angle measurements.

Fig. 10. Biface G15. 8084 – La vue des faces avec une carte colorimétrique permet de représenter les différences d'épaisseurde l'outil. Les vues de profil proviennent du modèle 3D. La localisation des différentes parties du bord est représentée par des lignes de couleur. Sections transversales et longitudinales et mesure des angles d'aiguisage.

of the operator to maintain a longitudinal cutting function until the depletion of the bifacial structure.

The three bivalent edges and two CEs present a functional configuration adapted to use for transversal cutting motions. In the case of the bivalent edge, this function is associated with another function: in one case with a CE/PE pair adapted to longitudinal cuts and in two cases with a tool for transverse cutting. This latter example only concerns a single biface: F14. 3242, which has a CE for transverse cutting and two bivalent edges. The functional potentialities of the two bivalent edges and the CE are not the same due to the convergence of the CE and the rectilinear or notched morphology of the bivalent edge. This biface is the only one of the series with functional potentialities for transversal cutting.

The distribution of the different CE/PE pairs among the bifaces is as follows: five bifaces have longitudinal cutting potential, four of which only have this potential and one also has a CE/PE pair for transversal cutting. One of these bifaces has three pairs of CE/PE destined for longitudinal cuts (E13. 2546). A single biface only presents transversal cutting potential (F13. 3242). Indeed, the main functional configuration is for shallow or deep longitudinal cuts. According to microwear studies, cutting activities are the main activity associated with Acheulean bifaces, in particular, cutting meat (García-Medrano et al., 2014; Keeley, 1980; Lhomme et al., 2004; Mitchell, 1998; Ollé, 2003), or ligneous (Binneman and Beaumont, 1992) and non-ligneous plants (Lhomme et al., 1998).

This use seems to be linked to a specific morphological configuration associating a cutting edge and a pointed apical extremity, allowing the biface to penetrate into the material in order to incise it more and more deeply. This functional configuration of the cutting edge, associated with the cutting activities in this study, is also interpreted in the same way in former works (Albrecht and Müller-Beck, 1988; Ollé, 2003), where it is associated with a much thicker prehensile base. The association of a thick, non-cutting base and a transformative part with a closed angle, a long cutting edge and a point, is considered by certain authors the optimal distribution of the mass for cutting activities (Gowlett, 2006; Simao, 2002). Consequently, the bifaces from level P3 from the "Caune de l'Arago" support the postulate that these tools were used for longitudinal cutting.

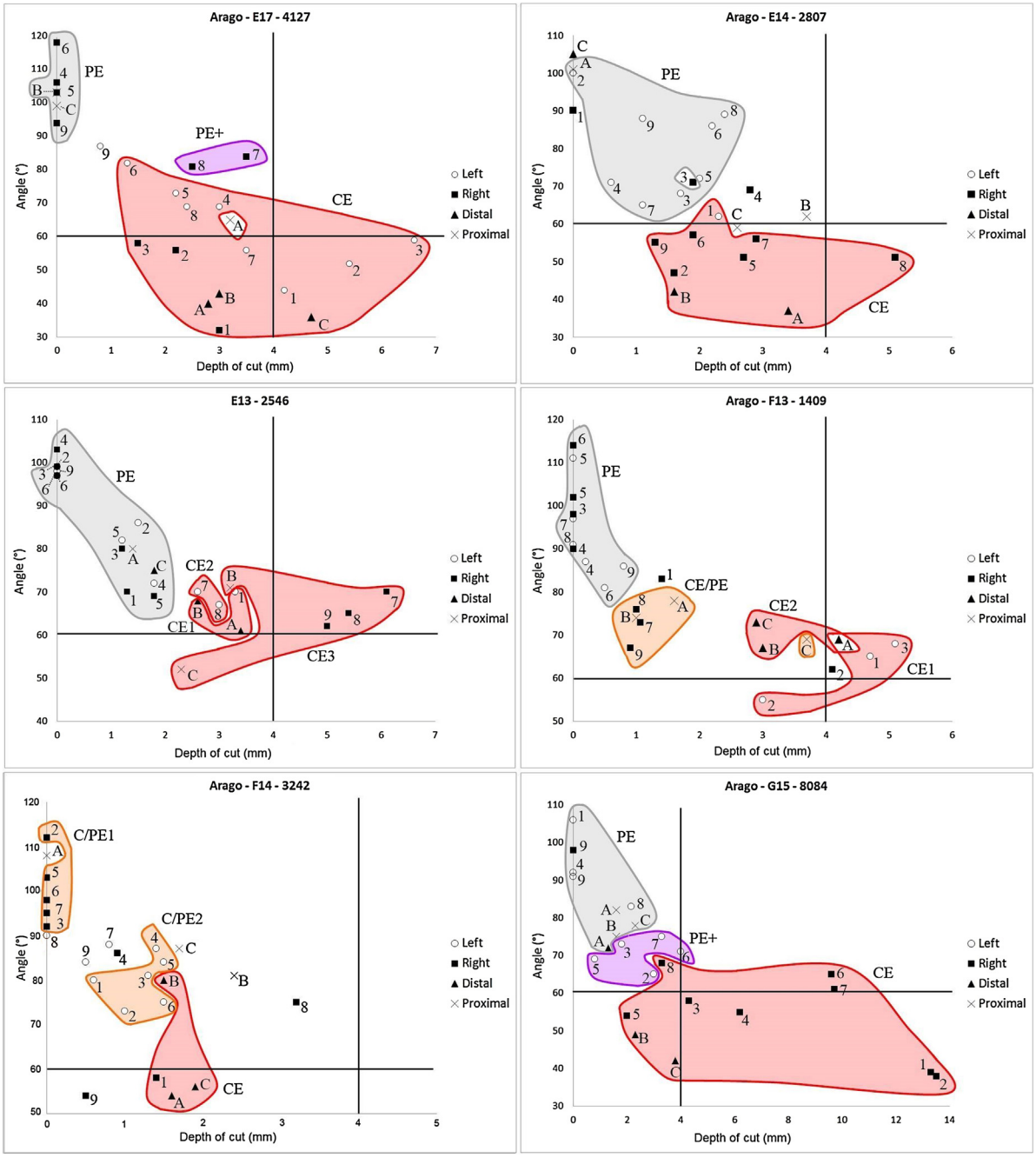

Fig. 11. Bivariate diagrams with edge angle (on the vertical axis) and depth of section (on the horizontal axis) for the six bifaces from AU P3. A line at 60° and another at 4 mm, highlight the variability of the potential functions of bifaces (numbers correspond to the location of the section, visible on Figs. 5 and 6).
Fig. 11. Diagrammes bivariés avec l'angle d'affûtage (en ordonnée) et la profondeur de coupe (en abscisse) pour les 6 bifaces de l'UA P3. Une ligne est disposée à 60° et une autre à 4 mm, pour souligner la variabilité des fonctions potentielles des bifaces. (Les nombres correspondent à la localisation des sections, visibles sur les Fig. 5 et 6).

6. Conclusion

The use of three-dimensional biface models allows us to take accurate angle measurements of all the transverse sections. The contribution of the measurement of the depth of cut is particularly significant for distinguishing between the more or less incisive characteristics of the cutting edge. These measurements open new perspectives for the characterization of the different edges of a lithic tool and should enable us, in the long term, to clarify the functional choices made by Hominids. This measurement technique thus provides new graphic representations of the functional differences between bifaces.

This methodology characterizes the functional potential of bifaces, and in particular the distinction between transverse and longitudinal cutting tools. In addition, for longitudinal cutting groups, cutting edges can be more precisely correlated with deep cutting actions, which can be tangential or incisive. For the bifaces from level P3 from the "Caune de l'Arago", the results presented here mainly reveal longitudinal cutting potential. This type of action is the most commonly recorded movement by microwear studies, which tends to confirm the informative potential of the methodology presented in this work.

In light of these results, this method could be applied to other Middle Pleistocene series of bifaces and should also allow us to explain the variability of these tools. It would also be interesting to test the informative potential of this methodology for other types of tools, such as choppers, picks and cleavers.

Acknowledgments

The acquisition of three-dimensional biface models forms the practical basis of this work. I wish to thank the engineers and technicians of the "Centre européen de recherche préhistorique de Tautavel" for their participation: M. Quaterpoint, C. Planchand, and C. Fontaneil. Thanks to H. De Lumley for providing access to the collections of Arago Cave. Thanks also to G. Becam for teaching us how to use the Avizo software and to L. Byrne (official translator) for the translation. I wish to thank L. Bourguignon and H. Forestier for their reviews and comments, which enhanced the first draft of this paper. Thanks also to the anonymous reviewers for their pertinent comments, which improved this article.

References

Abel, R.L., Parfitt, S., Ashton, N., Lewis, G.-S., Scott, B., Stringer, C., 2011. Digital preservation and dissemination of ancient lithic technology with modern micro-CT. Comput. Graph. 35/4, 878–884.

Albrecht, G., Müller-Beck, H., 1988. The Palaeolithic of Sehremuz near Samsat on the Euphrates river. Summary of the excavation findings and a morphology of the handaxes. Paleorientology 14 (2), 76–86.

Atkins, T., 2009. The Science and engineering of cutting: the mechanics and processes of separating, scratching and puncturing biomaterials, metals and non-metals. Butterworth-Heinemann.

Barsky, D., 2013. The Caune de l'Arago stone industries in their stratigraphical context. C. R. Palevol 12, 305–325.

Bertrand, A.-J., Bertrand, B., 1997. Jean de Pyréne, rémouleur François. Suivi d'un cahier pratique d'aiguisage domestique. Le Savoir-Geste (176 p.).

Beyries, S., 1993. Are we able to determine the function of the earliest Palaeolithic tools? In: Berthelet, A., Chavaillon, J. (Eds.), The use of tool by human and non-human primates. Oxford Clarendon Press, pp. 225–236.

Binneman, J., Beaumont, P., 1992. Use-wear analysis of two Acheulean handaxes from Wonderwerk Cave, Northern Cape. S. Afr. Field Archaeol. 1, 92–97.

Boëda, E., 2013. Techno-logique & Technologie. Une Paléo-histoire des objets lithiques tranchants. Archéoéditions, Préhistoire au présent (266 p.).

Bordes, F., 1961. Typologie du Paléolithique ancien et moyen. Ed. Delmas, Bordeaux, France (85 p.).

Boucard, D., 2005. Les outils taillants. Jean-Cyrille Godefroy (281 p.).

Bretzke, K., Conard, N., 2012. Evaluating morphological variability in lithic assemblages using 3D models of stone artifacts. J. Achaeol. Sci. 39, 3741–3749.

Cabanié, H., 1932. Manuel de coutellerie. Émotion Primitive Éditions (242 p.).

Chacon, M.-G., Detroit, F., Coudeneau, A., Moncel, M.-H., 2016. Morphometric Assessment of Convergent Tool Technology and Function during the early Middle Palaeolithic: The case of Payre, France. Plos One, 1–20.

Clarkson, C., Hiscock, P., 2011. Estimating original flake mass from 3D scans of platform area. J. Archaeol. Sci. 38, 1062–1068.

Cornford, J.-M., 1986. Specialized resharpening techniques and evidence of handedness. In: Callow, P., Cornford, J.-M. (Eds.), La Cotte de St. Brelade. 1961–1978. Excavations by C.B.M. McBurney. Geo Books, Norwich, pp. 337–351.

Dibble, H., Bernard, M., 1980. A comparison of basic edge angle measurement techniques. Am. Antiquity 45, 857–865.

Falguères, C., Shao, Q., Han, F., Bahain, J.J., Richard, M., Perrenoud, C., Moigne, A.M., de Lumley, H., 2015. New ESR and U-series dating at Caune de l'Arago, France: A key-site for European middle Pleistocene. Quat. Geochron. 30, 547–553.

García-Medrano, P., Ollé, A., Mosquera, M., Cáceres, I., Díez, C., Carbonell, E., 2014. The earliest Acheulean technology at Atapuerca (Burgos, Spain): Oldest levels of the Galería site (GII Unit). Quat. Int., 170–174.

Geneste, J.-M., Plisson, H., 1996. Production et utilisation de l'outillage lithique dans le Moustérien du Sud-Ouest de la France : Les Tares à Sourzac, vallée de l'Isle, Dordogne. In: Bietti, A., Grimaldi, S. (Eds.), Reduction processes for the European Mousterian. Colloque de Rome, Quaternaria Nova VI, pp. 343–367.

Gould, A.-R., Koster, D.-A., Sontz, A.-H.-L., 1971. The lithic assemblage of the western desert Aborigines of Australia. Am. Antiquity 36/2, 149–169.

Gowlett, J.A.J., 2006. The early settlement of northern Europe: Fire history in the context of climate change and the social brain., pp. 299–310.

Grégoire, S., 2000. Origine des matières premières des industries lithiques du Paléolithique pyrénéen et méditerranéen. Contributions à la connaissance des aires de circulations humaines. PhD thesis. Université de Perpignan (1 vol., 246 p., ill).

Hayden, B., 1977. Stone tool functions in the Western Desert. In: Wright, R.V.S. (Ed.), Stone Tools as Cultural Markers. Humanities Press, New Jersey, pp. 178–188.

Hayden, B., 2015. Insights into early lithic technologies from ethnography. Phil. Trans. R. Soc. B 370 (7 p.).

Keeley, L.H., 1980. Experimental determination of stone tool use. University of Chicago Press, Chicago, IL, USA (209 p.).

Key, A.-J.-M., 2016. Integrating Mechanical and Ergonomic Research within Functional and Morphological Analyses of Lithic Cutting Technology: Key Principles and Future Experimental Directions. Ethnoarchaeology, 1–21.

Key, A.-J.-M., Lycett, S.-J., 2015. Edge angle as a variably influential factor in flake cutting efficiency: an experimental investigation of its relationship with tool size and loading. Archaeometry 57, 911–927.

Key, A.-J.-M., Lycett, S.-J., 2017a. Influence of Handaxe Size and Shape on Cutting Efficiency: A Large-Scale Experiment and Morphometric Analysis. J. Archaeol. Method Theory 24, 514–541.

Key, A.-J.-M., Lycett, S.-J., 2017b. Form and function in the Lower Palaeolithic: history, progress, and continued relevance. J. Anthropol. Sci. Invited Rev. 95, 1–42.

Key, A.-J.-M., Proffitt, T., Stefani, E., Lycett, S.-J., 2016. Looking handaxes from another angle: Assessing the ergonomic and functional importance of edge form in Acheulean bifaces. J. Anthropol. Archaeol. 44, 43–55.

Klaric, L., Lev, S., Giria, Y., Polanskà, M., 2015. Couteaux de Kostienki et lames aménagées par technique de Kostienki : retour sur un malentendu historique. Bull. Soc. Prehist. Fr. 112–3, 421–474.

Lemorini, C., 1992. Variabilité ou spécialisation fonctionnelle? Une révision du rapport entre forme et fonction au Moustérien. Analecta Praehistorica Leidensia 25, 17–24.

Lepot, M., 1993. Approche techno-fonctionnelle de l'outillage moustérien. Essai de classification des parties actives en termes d'efficacité technique. Application à la couche M2e sagittale du Grand Abri de la Ferrassie (fouilles H. Delporte). Mémoire de maîtrise. Université Paris-10, Nanterre (159 p.).

Leroi-Gourhan, A., 1943. L'Homme et la matière. Albin Michel, Paris (352 p.).

Leroi-Gourhan, A., 1964. Le geste et la parole. Tome I. Technique et langage. Albin Michel, éditions Sciences d'aujourd'hui (1988 edition ; 323 p.).

Lhomme, V., Bemilli, C., Beyries, S., Christensen, M., Connet, N., 1998. Soucy 1 (Yonne) : interprétations et réflexions sur un site du Pleistocène moyen en contexte alluvial. In: Brugal, J.-P., Meignen, L., Patou-Mathis, M. (Eds.), Économie préhistorique : les comportements de subsistance au Paléolithique. Actes des XIIIes Rencontres internationales d'archéologie et d'histoire d'Antibes, APDCA, Sophia Antipolis. , pp. 259–271.

Lhomme, V., Connet, N., Chaussé, C., Bémilli, C., Bahain, J.-J., Voinchet, P., 2004. Les sites et les industries lithiques du Paléolithique inférieur, moyen et supérieur de la basse vallée de l'Yonne dans leurs contextes chronostratigraphiques. Bilan de dix ans d'activité archéologique pluridisciplinaire dans le Sud-Est du Bassin parisien. Bull. Soc. Prehist. Fr. 101 (4), 701–739.

Li, H., Kuman, K., Li, C., 2016. The symmetry of handaxes from the Danjiangkou Reservoir Region (central China): A methodological consideration. Quat. Int. 400, 65–72.

de Lumley, H. (Ed.), 2015. Caune de l'Arago Tome VI Tautavel-en-Roussillon, Pyrénées-Orientales, France : Individualisation des unités archéostratigraphiques. Tome VI. CNRS Éditions, Paris (642 p.).

Machin, A.-J., Hosfield, R.-T., Mithen, S.-J., 2007. Why are some handaxes symmetrical? Testing the influence of handaxe morphology on butchery effectiveness. J. Archaeol. Sci. 34, 883–893.

Mansur-Franchomme, M.-E., 1986. Microscopie du matériel lithique préhistorique : traces d'utilisation, altérations naturelles, accidentelles et technologiques. Exemples de Patagonie. Cah. Quaternaire 9 (286 p.).

Marquez, B., Ollé, A., Sala, R., Verges, J.-M., 2001. Perspectives méthodologiques de l'analyse fonctionnelle des ensembles lithiques du Pléistocène inférieur et moyen d'Atapuerca (Burgos, Espagne). L'Anthropologie 105, 281–299.

McGorry, W.-R., Dowd, C.-P., Dempsey, G.-P., 2003. Cutting moments and grip forces in meat cutting operations and the effect of knife sharpness. Appl. Ergon. 34 (4), 375–382.

McGorry, W.-R., Dowd, C.-P., Dempsey, G.-P., 2005. The effect of blade finish and blade edge angle on forces used in meat cutting operations. Appl. Ergon. 36 (1), 71–77.

Mitchell, J.-C., 1998. A use-wear analysis of selected British Lower Paleolithic Handaxes with special reference to the site of Boxgrove (West Sussex). A study incorporating optical 378 microscopy, computer aided image analysis and experimental archaeology. PhD thesis. Somerville College, Oxford, UK (604 p.).

Moncel, M.-H., 1995. Biface et outil-biface du Paléolithique moyen ancien réflexion à partir des sites d'Ardèche Orgnac 3 et Payre. Paleo 7, 157–169.

Morales, J.-L., Lorenzo, C., Vergès, J.-M., 2015. Measuring retouch intensity in lithic tools: a new proposal using 3D scan data. J. Archeol. Method Theory 22 (2), 543–558.

Ollé, A., 2003. Variabilitat i patrons funcionals en els sistemes tècnics de Mode 2. Anàlisi de les deformacions d'úsen els conjunts lítics del Riparo Esterno de Grotta Paglicci (Rignano Garganico, Foggia), Áridos (Arganda, Madrid) i Galería-TN (Sierra de Atapuerca, Burgos). Thèse. Universitat Rovira i Virgili, Tarragona, Spain (580 p.).

Ollé, A., Vergès, J.-M., Peña, L., Aranda, V., Canals, A., Carbonell, E., 2012. A microwear analysis of Handaxes from Santa Ana Cave (Caceres, Extremadura, Spain). In: Marreiros, J., Bicho, N., Gibaja, J.-F. (Eds.), International Conference on Use-Wear Analysis. Use-Wear. , pp. 270–278.

Raynaud, M., 2010. Étude du potentiel fonctionnel des bifaces en silex du site Paléolithique inférieur de la caune de l'Arago (Pyrénées-Orientales, France). Memoire de Master 2. Université Perpignan Via-Domitia, Perpignan, France (121 p.).

Roe, D.-A., 1981. The Lower and Middle Palaeolithic Periods in Britain. Routledge et Kegan Paul, London, Boston and Henley (324 p.).

Rots, V., Van Peer, P., 2006. Early evidence of complexity in lithic economy: core-axes production, hafting and use at late middle Pleistocene site 8-B-11, Sai Island (Sudan). J. Archaeol. Sci. 33, 360–371.

Schick, K.-D., Toth, N., 1993. Making silent Stones Speak. TouchStone Book, New York (352 p.).

Siegel, P., 1985. Edge angle as a functional indicator: a test. Lithic Technol. 14 (2), 90–94.

Simao, J., 2002. Tools evolve: the artificial selection and evolution of Paleolithic stone tools. Behav. Brain Sci. 25 (3), 419.

Singh, V., Das, M., Kumar Das, S., 2016. Effects of knife edge angle and speed on peak force and specific energy when cutting vegetables of diverse texture. Int. J. Food Stud. 5, 22–38.

Soladenko, N., Zupancich, A., Nunziante Cesaro, S., Marder, O., Lemorini, C., Barkai, R., 2015. Fat Residue and Use-Wear Found on Achuelian Biface and Scraper Associated with butchered Elephant Remains at the Site of Revadim, Israel. Plos One 10 (3) (17 p.).

Soressi, M., 2002. Le Moustérien de tradition acheuléenne du Sud-Ouest de la France. Discussion sur la signification du faciès à partir de l'étude comparée de quatre sites : Pech-de l'Azé I, Le Moustier, La Rochette et la Grotte XVI. Thèse. Université Bordeaux-1, Bordeaux, France (330 p.).

Soriano, S., 2000. Outillage bifacial et outillage sur éclat au Paléolithique ancien et moyen, coexistence et interaction. Université Paris-10, pp. 460 p, Thèse.

Terradillos-Bernal, M., Rodriguez, X.-P., 2012. The Lower Palaeolithic on the northern of the Iberian Peninsula (Sierra de Atapuerca, Ambrona and La Maya I): a technological analysis of the cutting edge and weight of artefacts. Developing an hypothetical model. J. Archaeol. Sci. 39, 1467–1479.

Tringham, R., Cooper, G., Odell, G., Voytek, B., Whitman, A., 1974. Experimentation in the Formation of Edge Damage. A New Approach to Lithic Analysis. J. Field Archaeol. 1, 171–196.

Vayson de Pradennes, A., 1937. Les dénominations de l'outillage du Paléolithique inférieur. Revue Anthropologique 4–6, 91–112.

Viallet, C., 2016a. Bifaces used for percussion? Experimental approach to percussion marks and functional analysis of the bifaces from Terra Amata (Nice, France). Quat. Int. 409, 174–181.

Viallet, C., 2016b. Macrotraces of middle Pleistocene bifaces from two Mediterranean sites: Structural and functional analysis. Quat. Int. 411 (Pt B), 202–211.

Viallet, C., 2016c. Potentiel fonctionnel des outils bifaciaux au Pléistocène moyen en contexte méditerranéen. Analyse de la structure et des macro-traces des séries bifaciales de la caune de l'Arago, Terra Amata, Orgnac 3 et le Lazaret. Université de Perpignan-Via-Domitia, Perpignan, France, pp. 397 p, Thèse.

Wenban-Smith, F., Bridgland, D., 2001. Palaeolithic Archaeology at the Swan Valley Community School, Swanscombe. Kent. Proc. Prehist. Soc. 67, 219–259.

Wilmsen, E.-N., 1968. Functional analysis of flaked stone artefacts. Am. Antiquity 33, 156–161.